

Feedback-prop: Convolutional Neural Network Inference under Partial Evidence

Tianlu Wang¹, Kota Yamaguchi², Vicente Ordonez¹

¹University of Virginia, ²CyberAgent, Inc.

yamaguchi.kota@cyberagent.co.jp

{tw8cb, vicente}@virginia.edu

Abstract

In this paper, we propose an inference procedure for deep convolutional neural networks (CNNs) where partial evidence might be available during inference. We introduce a general feedback-based propagation approach (feedback-prop) that allows us to boost the prediction accuracy of an existing CNN model for an arbitrary set of unknown image labels when a non-overlapping arbitrary set of labels is known. We show that existing models trained in a multi-label or multi-task setting can readily take advantage of feedback-prop without any retraining or fine-tuning. This inference procedure also enables us to evaluate empirically various CNN architectures for the intermediate layers with the most information sharing with respect to target outputs. Our feedback-prop inference procedure is general, simple, reliable, and works on different challenging visual recognition tasks. We present two variants of feedback-prop based on layer-wise, and residual iterative updates. We perform evaluations in several tasks involving multiple simultaneous predictions and show that feedback-prop is effective in all of them. In summary, our experiments show a previously unreported and interesting dynamic property of deep CNNs, and presents a technical approach that takes advantage of this property for inference under partial evidence for general visual recognition tasks.

1. Introduction

In this paper we tackle visual recognition problems where partial evidence or partial information about the input image is available. For instance, if we know for certain that an image was taken at the *beach*, this should change our beliefs about the types of objects that could be present in the image, e.g. co-occurrence of an *office chair* is unlikely. This is because something is *known* for certain about the image even before performing any visual recognition. We argue that this setting is realistic in many applications, for instance images on the web are usually surrounded by text that provides some related information, images on social media

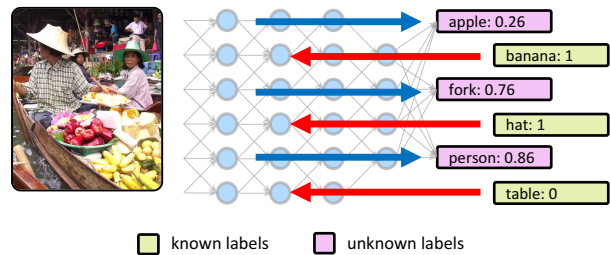


Figure 1: Our proposed feedback-based inference uses an arbitrary set of partial annotations as *known* labels to iteratively predict a set of *unknown* labels for each input sample during inference. This example shows a multi-label classification task. Neural activations are used to transfer information among variables in the target space.

have associated user comments, many images contain geo-location information, images taken with portable devices usually contain other sensor information. More generally, images in standard computer vision datasets are effectively partially annotated with respect to a single task or modality. Assuming only visual content as inputs, while convenient for benchmarking purposes, does not reflect many end-user applications where extra information is available during inference. We propose here a general framework to tackle this problem in any task involving deep convolutional neural networks trained with multiple target outputs or multiple tasks. We provide an example in Figure 1, where a set of labels are *known*: banana, hat, table, and we are trying to predict the other labels: apple, fork, person.

Convolutional neural networks (CNNs) have become the state-of-the-art in most visual recognition tasks. Their extraordinary representation power has allowed researchers to address problems at an unprecedented scale with remarkable accuracy. While reasoning under partial evidence using probabilistic graphical models would involve marginalizing over the variables of interest, CNNs do not model a joint distribution, therefore making such type of reason-

ing non-trivial. The typical pipeline using CNNs involves training the model using stochastic gradient descent (SGD) and the back-propagation algorithm [24] using an annotated dataset, and then performing forward-propagation during inference given only the visual input. In this paper, we challenge this prevailing inference procedure in CNNs where information only flows in one direction, and the model structure is static and fixed after training. We propose instead feedback-based propagation (feedback-prop) where forward and backward-propagation steps share information among neural units during inference, and where residual units –not present during training– are optionally incorporated. We show the effectiveness of our approach on multi-label prediction under incomplete and noisy labels, and multi-task learning with partial evidence for various datasets and tasks.

Our main hypothesis is that by *correcting* an intermediate set of neural activations in order to minimize the loss with respect to a set of *known* labels for an individual input sample, we would also be able to predict more accurately a complement set of *unknown* labels for that input sample. We demonstrate this behavior with feedback-prop for multiple tasks and under multiple CNN models and settings. There is notable evidence in previous research aimed at interpreting intermediate representations in CNNs showing that they encode basic patterns of increasing visual complexity (i.e. edges, attributes, object parts, objects) that are shared among target outputs [27, 33, 8, 30, 2]. Since the underlying shared representations of the network capture common patterns among the target outputs, they act as pivoting variables to transfer knowledge in the target space. We show that feedback-prop is general, simple to implement, and can be readily applied to a variety of problems with multiple simultaneous output predictions.

Our contributions can be summarized as follows:

- A general feedback-based propagation inference procedure (feedback-prop) for CNN prediction under partial evidence.
- Two variants of feedback-prop using layer-wise feedback updates, and residual feedback updates, and experiments showing their effectiveness on both multi-label and multi-task settings, including an experiment using in-the-wild web data.
- An extensive analysis of CNN architectures regarding optimal layers in terms of information sharing with respect to target variables.

2. Related Work

Context in Computer Vision Using contextual cues for visual recognition tasks has been long studied in the psychology literature [21, 20, 3, 6, 1], and some of these insights have also been utilized in computer vision [22, 10,

7, 19]. However, unlike our paper, most previous work using context still assume no extra information about images during inference. The contextual information is predicted jointly with the target predictions, and is often used to impose structure in the target space based on learned priors or statistics. In contrast, in our work we rely on the underlying contextual relations that are already implicitly encoded in a trained CNN, and we exploit them only during inference.

Multi-task Learning Another form of using context is by jointly training for multiple correlated visual recognition tasks [23, 31, 17], or multi-task learning, where knowledge about one task helps another target task. Our method is complementary and can directly be used with any of these models when extra information is available for at least one of the tasks or modalities. Unlike conditional models that require a fixed conditional input, our approach may be used with an arbitrary number of observations.

Optimizing the Input Space In terms of technical content, our proposed method has rather connections to previous works that optimize over inputs. This is common for tasks that require modifying or generating an image. One prominent example is the iterative approach employed to generate adversarial examples constructed to fool a CNN model [13]. This style of gradient-based optimization over inputs is also leveraged for the task of style transfer where the objective is to iteratively modify an image to use the style of another image [11]. Gradients over inputs are also used as the supervisory signal in the generator network of Generative Adversarial Networks (GANs) [12]. Gradient-based optimization has also been used to visualize the intermediate representations learned by a deep CNN, or to identify the regions that are mostly influencing target predictions [27, 5, 32, 34, 25, 4]. However, unlike those methods, our focus is still on the target predictions and not the inputs, and changing the underlying activations, or inputs of the model is used only as a means toward improving the target predictions. In our approach, the input image space might not be the optimal representation where shared information among target predictions is maximal. We actually find that CNN layers that lie somewhere in the middle are more beneficial.

Inference under Partial Annotations A relevant recent experiment regarding task setup was proposed in Hu et al [15]. This work introduces a novel deep CNN architecture that can be adapted to a setting where partial labels are *known* during test time. The paper presents an experiment where fine-grained attribute labels are predicted given an input image and a set of *known* coarse scene categories. In our work, we do not propose a new CNN model but instead an inference procedure that can be readily applied to any off-the-shelf pre-trained CNN that works for an arbitrary set of target variables.

3. Method

This section presents our feedback-based inference procedure. We start from the derivation of our most basic *single-layer feedback-prop* inference (section 3.1), and introduce our two more general versions: *layer-wise feedback-prop* (LF) (section 3.2), and our more efficient *residual feedback-prop* (RF) (section 3.3).

3.1. Feedback-based Inference

Let us consider a scenario where we have a feed-forward CNN already trained to predict multiple outputs for either a single task or multiple tasks. Let $\hat{Y} = F(X, \Theta)$ represent our trained CNN, where X is an input image, \hat{Y} is a predicted set of labels, and Θ are the model parameters. Now, let us assume some labels are given at the inference time, and split the label variables into *known* and *unknown*: $Y = (Y_k, Y_u)$. The neural network by default makes a joint prediction for both sets of variables: $\hat{Y} = (\hat{Y}_k, \hat{Y}_u) = (F_k(X, \Theta), F_u(X, \Theta))$. Given the *known* set of true values Y_k , we can compute a partial loss only with respect to this set for input sample X as $L(Y_k, \hat{Y}_k)$. The key idea behind feedback-prop is to back-propagate this partially observed loss to the network, and iteratively update the input X in order to re-compute the predictions on the set of *unknown* variables Y_u . Formally, our feedback-based procedure can be described as follows:

$$X^* = \operatorname{argmin}_X L(Y_k, F_k(X, \Theta)), \quad (1)$$

$$\hat{Y}_u^* = F_u(X^*, \Theta), \quad (2)$$

where we optimize X and forward-propagate to compute refined *unknown* labels \hat{Y}_u^* . In fact, we need not be restricted to iteratively update X but any arbitrary intermediate representation in any layer. Let us denote the l -th unit's internal neural activation of the network as a_l , and the dissected network at unit l by $Y = F^{(l)}(a_l)$, which can be interpreted as a truncated forward propagation in the original network from layer l until the prediction layer. Then, we can proceed as follows:

$$a_l^* = \operatorname{argmin}_{a_l} L(Y_k, F_k^{(l)}(a_l, \Theta)), \quad (3)$$

$$\hat{Y}_u = F_u^{(l)}(a_l^*, \Theta). \quad (4)$$

In this formulation, we have the option of optimizing intermediate representations at an arbitrary layer in the original model shared by F_k and F_u . Note that equation 1 is a special case of single-layer feedback-prop when using $a_0 \equiv X$. We show in Figure 2 a visual representation of this approach.

3.2. Layer-wise Feedback-prop (LF)

In this section, we propose a more general version of feedback-prop that leverages multiple intermediate representations in a CNN across several layers. Our layer-wise feedback-prop procedure minimizes a loss function

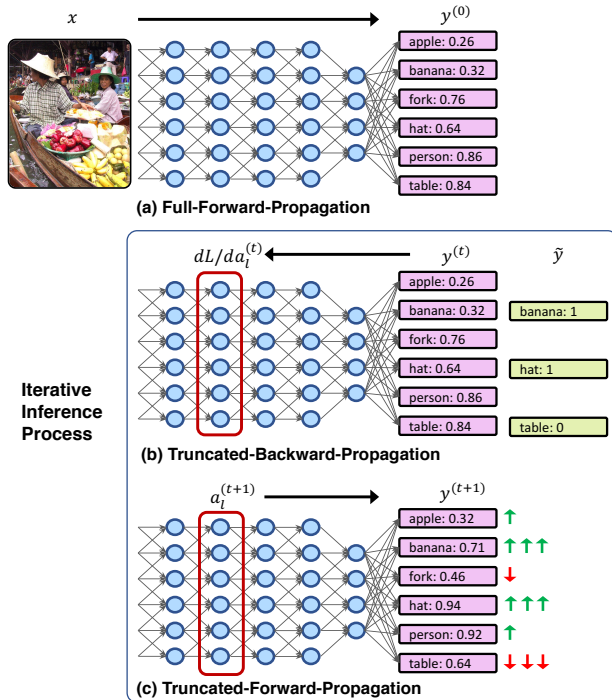


Figure 2: Overview of our approach. We propose a general feedback-based inference procedure (feedback-prop) for deep CNNs that leverages partial evidence during inference consisting of three basic steps (a) Full forward propagation, (b) truncated backward propagation and (c) truncated forward propagation.

$L(Y_k, F_k(A, \Theta))$ by optimizing a set of intermediate activations $A \equiv \{a_l, a_{l+1}, \dots\}$. However, in feed-forward models there is a dependency between internal representations, as a_l is needed to compute a_{l+1} . Therefore, optimizing multiple intermediate representations requires layer-by-layer sequential updates.

We describe *layer-wise feedback-prop* in detail in Algorithm 1. Forward represents a truncated forward propagation routine from the given input at a certain layer until the output layer, and Backward represents a truncated back-propagation of gradients from the output layer to an intermediate set of representations. Given an input image X , known values for variables Y_k , and a topologically sorted list of neural activation variables A , the algorithm optimizes internal representations a_l in topological order. The updates are performed in this fashion so that the algorithm *freezes* activation variable a_l layer-by-layer from the input side so that after each freeze, the next variable can be initialized to apply feedback updates. In Algorithm 1, λ is an update rate and iterative SGD steps are repeated T times. The update operation (line 7 of Algorithm 1) may be replaced by other types of SGD update rules such as SGD with momen-

Algorithm 1 Layer-wise Feedback-prop Inference

Require: Input image X , *known* labels \tilde{Y}_k , and a list of units $A \equiv \{a_l, a_{l+1}, \dots\}$

Ensure: Prediction \hat{Y}_u

- 1: $a_0^{(T)} := X$
 - 2: **for** $a_l \in A$ **do**
 - 3: $Y_k^{(0)}, a_l^{(0)} := \text{Forward}(a_{l-1}^{(T)})$
 - 4: **for** $t = 0$ **to** T **do**
 - 5: Compute the partial loss $L(\tilde{Y}_k, Y_k^{(t)})$
 - 6: $\frac{\partial L}{\partial a_l^{(t)}} := \text{Backward}(L)$
 - 7: $a_l^{(t+1)} := a_l^{(t)} - \lambda \frac{\partial L}{\partial a_l^{(t)}}$
 - 8: $Y_k^{(t+1)} := \text{Forward}(a_l^{(t+1)})$
 - 9: **end for**
 - 10: **end for**
 - 11: $\hat{Y}_u = \text{Forward}(a_N^{(T)})$
-

tum, AdaGrad, or Adam. Note that the backward, and forward propagation steps only go back as far as a_l , and do not require a full computation through the entire network. The *single-layer feedback-prop* inference in section 3.1 is a special case of *layer-wise feedback-prop* when $|A| = 1$. The choice of the set of layers will affect the ability of LF feedback-prop to improve the predictions for *unknown* target variables.

3.3. Residual Feedback-prop (RF)

The proposed *layer-wise feedback-prop* (LF) inference can use an arbitrary set of intermediate layer activations, but is inefficient due to the double-loop in Algorithm 1, where layers have to be updated individually in each pass. In this section, we refine our formulation even further by proposing a method that simulates updates to multiple intermediate layer representations in a single pass through the incorporation of auxiliary residual variables. We name this version of our inference procedure *residual feedback-prop* inference.

The core idea is to inject an additive variable (feedback residual) to intermediate representation variables, and optimize over residuals instead of directly updating the intermediate representations. Notice, that incorporation of these residual variables happens only during inference, and does not involve any modifications in the way the model was trained, or whether the underlying model uses residual units itself. We add a feedback residual variable r_l to the unit activation a_l in the forward propagation at layer l as follows:

$$a_l = f_l(a_{l-1}, \theta_l) + r_l, \quad (5)$$

where f_l is the original layer transformation function (e.g. convolutional filtering) at l with model parameters θ_l . When $r_l = 0$, this is a standard forward-propagation procedure. Instead of directly updating a_l by feedback-prop as in sec-

tion 3.2, we only update residual variables r_l . Figure 3 shows how residual variables are incorporated in a model during inference.

Algorithm 2 describes in detail how residual feedback-prop operates. The procedure starts by setting residuals to zero (line 1). The inner-loop is a truncated feed-forward propagation starting in activation a_l but using additive residuals. Notice that this computation does not incur in significant computational overhead compared to the original forward propagation. Optimization updates do not require a double-loop (lines 9-10), and therefore avoid the additional computational overhead of layer-wise feedback-prop inference that updates intermediate representations directly. We show in our experimental section that residual-based feedback-prop (RF) performs comparably to layer-wise feedback-prop (LF) in multi-label and multi-task models, and is comparably more efficient when updating multiple layers (section 6).

Algorithm 2 Residual Feedback-prop Inference

Input: Input image X , *known* labels \tilde{Y}_k , and a list of units $A \equiv \{a_l, a_{l+1}, \dots\}$

Output: Prediction \hat{Y}_u

- 1: $\mathbf{r}^{(0)} \equiv \{r_l^{(0)} | l \in \mathcal{L}\} := \mathbf{0}$
 - 2: $a_0 := X$
 - 3: **for** $t = 0$ **to** T **do**
 - 4: **for** $a_l \in A$ **do**
 - 5: $a_l^{(t)} := \text{Forward}(a_{l-1}^{(t)}) + r_l^{(t)}$
 - 6: **end for**
 - 7: $Y_k^{(t)} := \text{Forward}(a_N^{(t)})$
 - 8: Compute the observation loss $L(\tilde{Y}_k, Y_k^{(t)})$
 - 9: $\frac{\partial L}{\partial \mathbf{r}^{(t)}} := \text{Backward}(L)$
 - 10: $\mathbf{r}^{(t+1)} := \mathbf{r}^{(t)} - \lambda \frac{\partial L}{\partial \mathbf{r}^{(t)}}$
 - 11: **end for**
 - 12: $\hat{Y}_u = \text{Forward}(a_N^{(T)})$
-

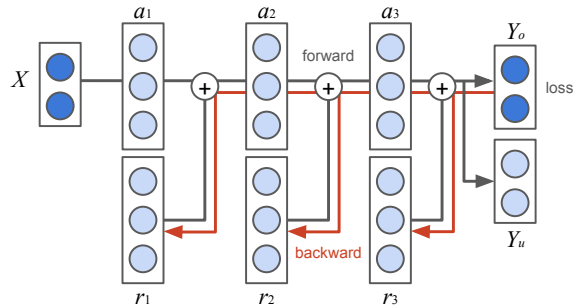


Figure 3: In RF feedback-prop, residual variables r_l are updated instead of intermediate activations a_l in order to avoid sequential dependencies and simulate intermediate representation updates for all layers in a single pass.

4. Experiments

We evaluate our approach on three tasks 1) Multi-label image annotation with incomplete labels, where incomplete labels are simulated at test time by artificially splitting the total set of labels into *known* and *unknown* (section 4.1), 2) Automatic annotation of news images in-the-wild, where surrounding news text is used as *known* evidence, and a set of visual words from image captions are used as *unknown* targets (section 4.2), and 3) A multi-task joint prediction of image captions and object categories, where the objective during inference is to predict image captions as the *unknown* target (section 4.3).

4.1. Multi-label Image Annotation

In our first experiment we use the COCO dataset [18], containing around 120k images, each annotated with 5 human-provided captions obtained using crowd-sourcing. We use the standard split in the dataset that has 82,783 images in the training set and subdivide the standard validation set into 20,000 images for validation and 20,504 for testing. Our task is to predict visual concepts for any given image. For this purpose, we first build a vocabulary of concepts using the most frequent words in the image captions. This task setting is similar to the visual concept classifier used by Fang et al [9]. We use all the captions in the training set after tokenization, lemmatization, and stop-word removal to build a vocabulary with the top 1000 most frequent words. We first train a multi-label prediction model by modifying a standard CNN to predict 1000 outputs, and train under independent logistic regressors using a loss function as follows:

$$L = - \sum_{i=1}^d \frac{1}{N} \sum_{j=1}^N \lambda_j [y_{ij} \log \sigma(f_j(I_i, \Theta)) + (1 - y_{ij}) \log(1 - \sigma(f_j(I_i, \Theta)))] \quad (6)$$

where $\sigma(x) = 1/(1 + \exp(-x))$, is the sigmoid function, and $f_j(I_i, \Theta)$ is the unnormalized output score for category j given image I_i and Θ are the model parameters of the underlying CNN. Intuitively each term in this loss function encourages the activation f_j to increase if the label $y_{ij} = 1$ or decrease it otherwise. The weight parameters λ_j count the contribution of each class j differently. These parameters are designed to handle the extreme class imbalance that happens multi-label image annotation, a higher value of lambda is assigned to classes that occur less frequently. We particularly set $\lambda_j = \sum_{i=1}^{|D|} (1 - y_{ij}) / \sum_{i=1}^{|D|} y_{ij}$.

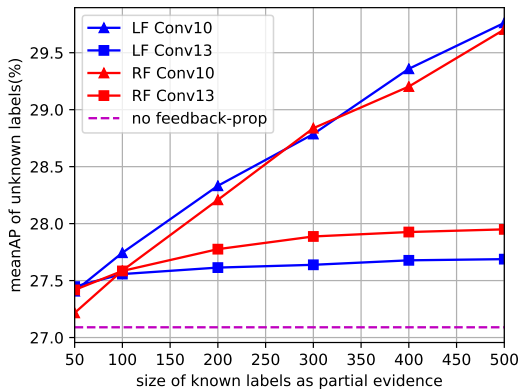
In order to evaluate feedback-prop quantitatively, we set aside a fixed set of 500 *unknown* target outputs during inference. We measure the mean average precision (area under the precision-recall curve) on this set as we experiment with different amounts of *known* labels, from 50 labels to

the total remaining of 500 labels. We report in Figure 4 results for both layer-wise feed-backprop (LF), and residual feedback-prop (RF) using several intermediate representations for both a VGG-16 model [28], and a Resnet-18 model [14]. We determine the update rate parameter, and number of iterations using the validation split and then report results on the test split.

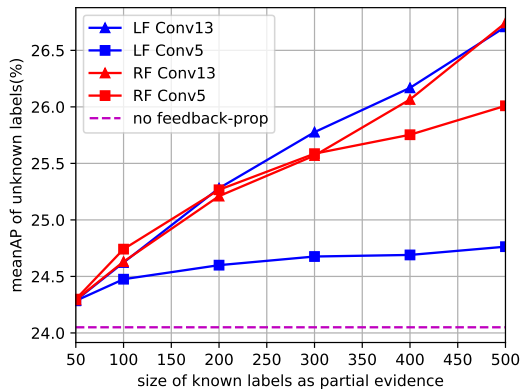
Observations: As we can observe, for both layer-wise feedback-prop (LF) and residual feedback-prop (RF), the prediction accuracy grows with larger amounts of partial evidence, and there does not seem to be any diminishing returns. This is exciting because as visual recognition systems learn to recognize a larger number of categories, an approach such as feedback-prop becomes more useful. Also, we can observe that different layer representations achieve different levels of accuracy, indicating that information shared with the target label space changes across internal convolutional layers in both residual (ResNet18) and non-residual CNNs (VGG-16). Figure 4(a) shows that VGG-16 achieves a meanAP on the set of *unknown* labels of 27.09 when using only the image as input and no partial evidence. This meanAP is consistently improved to 27.41 (on average) when only using a random sample of 50 *known* labels under layer-wise feedback-prop (LF) inference on the outputs of layer Conv13. Note that these 50 *known* labels are potentially unrelated to the 500 labels that the model is trying to predict, and most of them only provide weak negative evidence (e.g. $y_{ij} = 0$). When using the full complement set of 500 labels, the predictions achieve 29.76 meanAP, which represents a 9.8% relative improvement. Figure 4(b) shows that Resnet-18 achieves a meanAP of 24.05 using no additional evidence other than the input image. Residual feedback-prop (RF) using Conv13 can reach 26.74 given the non-overlapping set of 500 *known* labels as partial evidence, a relative improvement of 11.2%.

4.2. News Images Visual Concept Prediction

For this experiment, we first collect a dataset of news images with associated captions and news text from the BBC news website. Our resulting set contains 153,364 images for training, 10,213 images for validation and 10,307 images for testing. In this experiment, we train a multi-task model to jointly predict from a given image a set of visual concepts obtained from image captions, and a separate set of visual concepts obtained from surrounding news text. Both tasks are trained using the same multi-label loss and setup discussed in section 4.1. Here the vocabulary for the first task consists of the 500 most frequent nouns from image captions, and the vocabulary for the second task consists of the top 1,000 most frequent nouns from news texts. We use Resnet-50 [14] trained under the sum of the losses for each task. At inference time, we predict the visual concepts defined by words in the image captions (*unknown* la-



(a) Feedback-prop on VGG16



(b) Feedback-prop on ResNet18

Figure 4: Layer-wise feedback-prop inference (LF) and residual feedback-prop inference (RF) using different intermediate activations and increasing amounts of *known* labels in the COCO multi-label image annotation task.

bels), given the input image and the surrounding news text (*known* labels). We evaluate layer-wise feedback-prop (LF) using layer Conv40 and residual feedback-prop (RF) under Conv22. We find those layers to generally be the most useful under feedback-prop. We tune inference parameters such as number of iterations and update rates in the validation split and report results on the test split. Table 1 shows the meanAP across the set of *unknown* labels in the test split with varying amounts of additional partial evidence (surrounding news text).

Observations: The meanAP for predicting the set of *unknown* labels improves from 19.921% (only using input images) to 21.329% even when only using the first 25% of the surrounding news text as additional evidence. Using a larger portion of surrounding news text consistently increases the accuracy. When using all the available surrounding text for each news image the meanAP improves on average from 19.92% to 22.57%, a relative improvement of 13.3%. This is remarkable since –unlike our previous experiment– the surrounding text might also contain many confounding signals and noisy labels. We show qualitative examples by using layer-wise feedback-prop (LF) on Conv40 with all surrounding text in Figure 6 compared to image-only predictions.

4.3. Joint Captioning and Object Categorization

We train a multi-task CNN model on the COCO dataset [18] to jointly perform caption generation and multi-class object categorization. We use Resnet-50 with two additional separate output layers after the last convolutional layer, a multi-label prediction layer with 80-object outputs, and an LSTM branch for caption generation as in [29]. We shuffle images in the standard COCO train and validation splits and use 5000 images for validation and test, and the

	LF-conv-40	RF-conv-22
no-text	19.921	19.921
25% text	21.329	21.272
50% text	22.163	22.229
75% text	22.422	22.511
100% text	22.565	22.571

Table 1: Improvement of visual concept predictions on news images using surrounding news text.

remaining samples for training. We perform the same pre-processing of images and captions as in [16]. After training this multi-task model and evaluating on the validation split, it achieves a CIDEr score of 0.939 for the image captioning task, and a mean average precision score of 71.3% for object categorization. In order to evaluate feedback-prop in this experiment we use object annotations as *known* evidence and analyze the effects on the quality of the predicted image captions as our *unknown* labels. We use 20 iterations of feedback-prop with an update rate of 0.001. Table 5 presents results under this regime using the test split.

Observations: Feedback propagation between object annotations and intermediate convolutional layers or input images helps generate better image captions. When we use layer-wise feedback-prop on different activations, BLEU-4, ROUGE and CIDEr scores are all improved compared with no feedback-prop inference. Furthermore, we observe that updating multiple activations can outperform updating a single one in this experiment. Residual feedback-prop on Conv10 and Conv40 reaches the highest CIDEr score, improving from 0.9466 to 0.9922. It is important to note that this may not be the best performance feedback-prop can reach given object annotations since this experiment uses a fixed update rate and a fixed number of iterations, thus inter-

	LF	RF
no-fp	26.98	26.98
fp-input	29.14	29.53
fp-conv-1	29.72	29.56
fp-conv-4	29.65	29.66
fp-conv-7	29.77	29.79
fp-conv-10	29.82	29.74
fp-conv-13	27.59	27.87

Table 2: Layer by layer analysis of VGG-16 using Feedback-prop.

	LF	RF
no-fp	24.08	24.08
fp-input	24.74	27.06
fp-conv-1	24.16	25.91
fp-conv-5	24.57	25.76
fp-conv-9	25.94	26.71
fp-conv-13	26.80	27.26
fp-conv-17	24.19	24.22

Table 3: Layer by layer analysis of ResNet18 using Feedback-prop.

	LF	RF
no-fp	26.94	26.94
fp-input	28.35	29.28
fp-conv-1	27.60	29.49
fp-conv-10	29.54	29.80
fp-conv-22	29.61	29.89
fp-conv-40	29.71	29.67
fp-conv-49	27.14	27.14

Table 4: Layer by layer analysis of Resnet50 using Feedback-prop.

	BLEU-4	ROUGE	CIDEr
no-fp	28.65	0.5267	0.9466
LF-input	29.20	0.5290	0.9647
LF-conv-10	29.78	0.5333	0.9859
LF-conv-22	29.71	0.5327	0.9834
LF-conv-40	29.66	0.5332	0.9854
LF-conv-10, 40	29.73	0.5329	0.9872
RF-conv-10, 40	29.63	0.5337	0.9922

Table 5: Feedback-prop in multi-task learning: caption generation results benefit from object annotations as partial evidence using feedback-prop.

nal representation could be further updated by task-specific tuning of hyper-parameters.

5. What Layers are the Most Useful?

In previous experiments, we observe that benefit from partial evidence using feedback propagation varies when we update different intermediate activations. In this section, we seek to find where in the CNN are the most useful intermediate representations under feedback-prop. In other words, what are the intermediate layers of the network that seem to share maximal information with the target predictions. We first train three multi-label models based on Resnet-18, Resnet-50 and VGG-16 on the COCO multi-label task as described in section 4.1. Then we report for each model the best accuracy that can be reached by correcting a single layer activation using layer-wise feedback-prop (LF) and residual feedback-prop (RF). Results are reported in Table 2, 3, and 4. We observe that in both residual and non-residual CNNs, convolutional layers in the middle seem to share the most information with target space compared to layers closer to the input or layers closer to the output. Specifically, we find that Conv13 in ResNet18, Conv20 and Conv40 in ResNet-50, Conv7 and Conv10 in VGG-16 achieved the best performance given the same partial evidence during inference. Recent work instead analyzed neural networks using an information theory approach

where mutual information between intermediate representations with both inputs and outputs [26] is tracked during training. It would be interesting to analyze in future work the connection between information theory and the effectiveness of feedback-prop, perhaps those layers found to be useful under feedback-prop can be automatically determined using information theory instead of our exhaustive empirical approach.

6. Benchmarking Residual Feedback-prop

We can update multiple residual variables in a single back-propagation step which makes residual feedback-prop (RF) more efficient compared to layer-wise feedback-prop (LF). Here, we benchmark two proposed feedback-prop methods. We use the ResNet50 multi-label model trained in section 4.1 and select a sequence of activation layers including “input image”, “conv1”, “conv10”, “conv22”, “conv40”, “conv49”. Then we pick one layer as start layer and update this layer as well as all following layers. For example, if “conv40” is the start layer, “conv49” will also be updated. In this experiment, we use a single 12GB NVIDIA Pascal Titan X GPU and record average inference time per

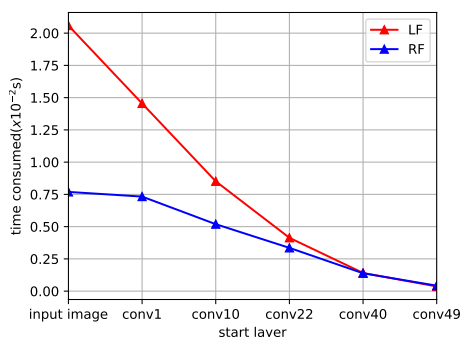


Figure 5: Benchmark results for layer-wise feedback-prop (LF) and residual feedback-prop (RF) inference. The x-axis shows the layer used for feedback-prop e.g. input_image is the most computationally intensive as it involves updating all subsequent layers.



no feedback-prop predictions:

claim:0.891679 try:0.592581 attack:0.278426 city:0.155168 hundred:0.133139 woman:0.120313 police:0.119733 report:0.104096	school:0.060947 people:0.054434 light:0.050388 part:0.045863 force:0.043337 area:0.042076 include:0.042012 security:0.039852	try:0.319411 show:0.186112 scene:0.158961 news:0.110425 people:0.092683 attack:0.059946 pay:0.050996 lead:0.049296	official:0.790290 home:0.310297 child:0.180287 people:0.139492 woman:0.088490 house:0.076746 camp:0.064999 use:0.063372	ceremony:0.506596 thousand:0.159579 pay:0.132895 game:0.104834 deal:0.080287 people:0.071572 open:0.048961 city:0.046278	people:0.494557 light:0.325617 launch:0.279506 sir:0.270729 point:0.243272 leave:0.150900 centre:0.133657 campaign:0.110601
--	---	---	---	---	--

with feedback-prop predictions:

claim:0.913860 attack:0.910921 bomb:0.267836 try:0.240699 body:0.159527 woman:0.123605 relative:0.121821 militant:0.119986	clash:0.948569 protester:0.774579 pro:0.520027 security:0.405497 force:0.176731 police:0.159598 anti:0.122141 government:0.064173	try:0.385340 protest:0.260692 medium:0.130189 china:0.119549 court:0.100340 show:0.086785 police:0.069903 woman:0.067833	camp:0.925969 refugee:0.908903 home:0.293703 child:0.255574 woman:0.147657 people:0.104480 syria:0.088542 official:0.061292	school:0.858543 game:0.284368 play:0.234772 thousand:0.112460 parent:0.085781 people:0.076458 start:0.061948 celebrate:0.058791	vote:0.488819 campaign:0.447369 people:0.388327 centre:0.309245 ireland:0.271122 leave:0.263814 point:0.179191 minister:0.133364
---	--	---	--	---	---

news text labels:

people, government, tell, police, country, state, group, report, find, place, school, public, news, attack, force, want, official, mean, support, death, security, put, use, leave, market, authority, office, claim, play, town, body, air, agency, india, past, ...	country, work, part, party, minister, report, number, school, leader, news, meet, house, force, court, power, want, official, end, council, support, election, death, security, use, win, university, street, vote, authority, office, fire, term, remain, prime, ...	people, government, tell, police, country, part, family, child, party, group, report, company, president, need, leader, public, news, business, house, help, force, court, case, member, want, official, china, set, death, security, hold, team, street, men, look, ...	action, start, fund, price, move, technology, syria, thousand, name, risk, offer, hope, saw, food, face, education, girl, act, crime, course, violence, crisis, book, age, return, france, organisation, space, access, try, hundred, provide, ...	union, today, secretary, offer, speak, key, executive, education, parent, development, stop, radio, energy, visit, mile, everyone, space, stage, club, opportunity, trust, department, sport, teacher, target, sir, commission, football, position, majority, ...	prime, start, statement, mark, station, act, person, age, return, ireland, morning, provide, island, couple, poll, candidate, referendum, amount, ask, voter, protect, date, proposal, bst, citizen, sex, difference, agree, one, limit, contract, count, ...
---	---	--	--	---	---

Figure 6: We show here qualitative examples from our News Image visual concept prediction task (second row), and our results obtained using layer-wise feedback-prop (LF) where words from surrounding news text (bottom row in blue) are used as partial evidence during inference (third row). Ground truth visual concept annotations for each image are highlighted in bold. Notice how the news text labels contain a variety of words that are only marginally relevant to the input images yet feedback-prop leverages this information effectively to improve the predictions. The surrounding news text provides high-level feedback that improves the predictions with concepts that would be hard to predict using image data alone.

image per iteration. Figure 5 shows that when more layers are updated during inference, residual feedback-prop (RF) shows the largest gains over layer-wise feedback-prop (LF).

7. Conclusions

In the context of deep CNNs, we found that by optimizing the intermediate representations for a given input sample during inference with respect to a subset of the target variables, all target variables improve accuracy. We proposed two variants of feedback-prop inference to leverage this dynamic property of CNNs and showed their effectiveness for making predictions under partial evidence for gen-

eral CNN models trained in a multi-label or multi-task setting. As multi-task models trained to solve a wide array of tasks such as UberNet [17] emerge, we expect feedback-prop will become increasingly useful. An interesting future direction would be devising an approach that also leverages feedback-based updates during training in order to improve the convergence or robustness of the learned visual representations of deep CNNs.

References

[1] M. Bar. Visual objects in context. *Nature Reviews Neuroscience*, 5(8):617–629, 2004. 2

- [2] D. Bau, B. Zhou, A. Khosla, A. Oliva, and A. Torralba. Network dissection: Quantifying interpretability of deep visual representations. In *CVPR*, 2017. 2
- [3] I. Biederman, R. J. Mezzanotte, and J. C. Rabinowitz. Scene perception: Detecting and judging objects undergoing relational violations. *Cognitive psychology*, 14(2):143–177, 1982. 2
- [4] A. Binder, G. Montavon, S. Bach, K.-R. Müller, and W. Samek. Layer-wise Relevance Propagation for Neural Networks with Local Renormalization Layers. *arXiv:1604.00825*, 2016. 2
- [5] C. Cao, X. Liu, Y. Yang, Y. Yu, J. Wang, Z. Wang, Y. Huang, L. Wang, C. Huang, W. Xu, et al. Look and think twice: Capturing top-down visual attention with feedback convolutional neural networks. In *ICCV*, pages 2956–2964, 2015. 2
- [6] M. M. Chun and Y. Jiang. Contextual cueing: Implicit learning and memory of visual context guides spatial attention. *Cognitive psychology*, 36(1):28–71, 1998. 2
- [7] S. K. Divvala, D. Hoiem, J. H. Hays, A. A. Efros, and M. Hebert. An empirical study of context in object detection. In *CVPR*, pages 1271–1278. IEEE, 2009. 2
- [8] V. Escorcia, J. C. Niebles, and B. Ghanem. On the relationship between visual attributes and convolutional networks. In *CVPR*, pages 1256–1264, 2015. 2
- [9] H. Fang, S. Gupta, F. N. Iandola, R. K. Srivastava, L. Deng, P. Dollár, J. Gao, X. He, M. Mitchell, J. C. Platt, C. L. Zitnick, and G. Zweig. From captions to visual concepts and back. In *CVPR*, pages 1473–1482, 2015. 5
- [10] C. Galleguillos, A. Rabinovich, and S. Belongie. Object categorization using co-occurrence, location and appearance. In *CVPR*, pages 1–8. IEEE, 2008. 2
- [11] L. A. Gatys, A. S. Ecker, and M. Bethge. Image style transfer using convolutional neural networks. In *CVPR*, pages 2414–2423, 2016. 2
- [12] I. Goodfellow, J. Pouget-Abadie, M. Mirza, B. Xu, D. Warde-Farley, S. Ozair, A. Courville, and Y. Bengio. Generative adversarial nets. In *NIPS*, pages 2672–2680, 2014. 2
- [13] I. J. Goodfellow, J. Shlens, and C. Szegedy. Explaining and harnessing adversarial examples. *arXiv preprint arXiv:1412.6572*, 2014. 2
- [14] K. He, X. Zhang, S. Ren, and J. Sun. Deep residual learning for image recognition. *CVPR*, 2016. 5
- [15] H. Hu, G.-T. Zhou, Z. Deng, Z. Liao, and G. Mori. Learning structured inference neural networks with label relations. In *CVPR*, pages 2960–2968, 2016. 2
- [16] A. Karpathy and L. Fei-Fei. Deep visual-semantic alignments for generating image descriptions. In *The IEEE Conference on Computer Vision and Pattern Recognition (CVPR)*, June 2015. 6
- [17] I. Kokkinos. Ubertnet: Training a ‘universal’ convolutional neural network for low-, mid-, and high-level vision using diverse datasets and limited memory. *CVPR*, 2017. 2, 8
- [18] T.-Y. Lin, M. Maire, S. Belongie, J. Hays, P. Perona, D. Ramanan, P. Dollár, and C. L. Zitnick. Microsoft coco: Common objects in context. In *ECCV*, pages 740–755. Springer, 2014. 5, 6
- [19] R. Mottaghi, X. Chen, X. Liu, N.-G. Cho, S.-W. Lee, S. Fidler, R. Urtasun, and A. Yuille. The role of context for object detection and semantic segmentation in the wild. In *CVPR*, June 2014. 2
- [20] D. Navon. Forest before trees: The precedence of global features in visual perception. *Cognitive psychology*, 9(3):353–383, 1977. 2
- [21] S. E. Palmer. The effects of contextual scenes on the identification of objects. *Memory & Cognition*, 3:519–526, 1975. 2
- [22] A. Rabinovich, A. Vedaldi, C. Galleguillos, E. Wiewiora, and S. Belongie. Objects in context. In *ICCV*, pages 1–8. IEEE, 2007. 2
- [23] W. Ruan and E. L. Miller. Ensemble multi-task gaussian process regression with multiple latent processes. *arXiv*, 2017. 2
- [24] D. E. Rumelhart, G. E. Hinton, and R. J. Williams. Learning representations by back-propagating errors. *Cognitive modeling*, 5(3):1, 1988. 2
- [25] R. R. Selvaraju, A. Das, R. Vedantam, M. Cogswell, D. Parikh, and D. Batra. Grad-cam: Why did you say that? visual explanations from deep networks via gradient-based localization. *arXiv preprint arXiv:1610.02391*, 2016. 2
- [26] R. Shwartz-Ziv and N. Tishby. Opening the black box of deep neural networks via information. *arXiv preprint arXiv:1703.00810*, 2017. 7
- [27] K. Simonyan, A. Vedaldi, and A. Zisserman. Deep inside convolutional networks: Visualising image classification models and saliency maps. *arXiv preprint arXiv:1312.6034*, 2013. 2
- [28] K. Simonyan and A. Zisserman. Very deep convolutional networks for large-scale image recognition. *ICLR*, 2015. 5
- [29] O. Vinyals, A. Toshev, S. Bengio, and D. Erhan. Show and tell: A neural image caption generator. In *CVPR*, 2015. 6
- [30] S. Vittayakorn, T. Umeda, K. Murasaki, K. Sudo, T. Okatani, and K. Yamaguchi. Automatic attribute discovery with neural activations. In *ECCV*, pages 252–268. Springer, 2016. 2
- [31] J. Wang, X. Zhu, S. Gong, and W. Li. Attribute recognition by joint recurrent learning of context and correlation. *arXiv*, 2017. 2
- [32] L. Xie, L. Zheng, J. Wang, A. L. Yuille, and Q. Tian. Interactive: Inter-layer activeness propagation. In *CVPR*, pages 270–279, 2016. 2
- [33] M. D. Zeiler and R. Fergus. Visualizing and understanding convolutional networks. In *ECCV*, pages 818–833. Springer, 2014. 2
- [34] J. Zhang, Z. Lin, S. X. Brandt, Jonathan, and S. Sclaroff. Top-down neural attention by excitation backprop. In *ECCV*, 2016. 2